Supplementary Information

Freestanding Symmetrical SiN/Si/SiN Composite Coated on Carbon Nanotube Paper for High-Performance Lithium-Ion Battery Anode Based on the Synergic Coupling Effects

Xinyi He[1, ‖], Fan Yue[1, ‖], Zhenzhen Shang[1], Jian Wang[1], Wenhua Gu[*, 2], Xiaodong Huang[*, 1]

Electronic mail: xdhuang@seu.edu.cn[*, 1], guwenhua@njust.edu.cn[*, 2].

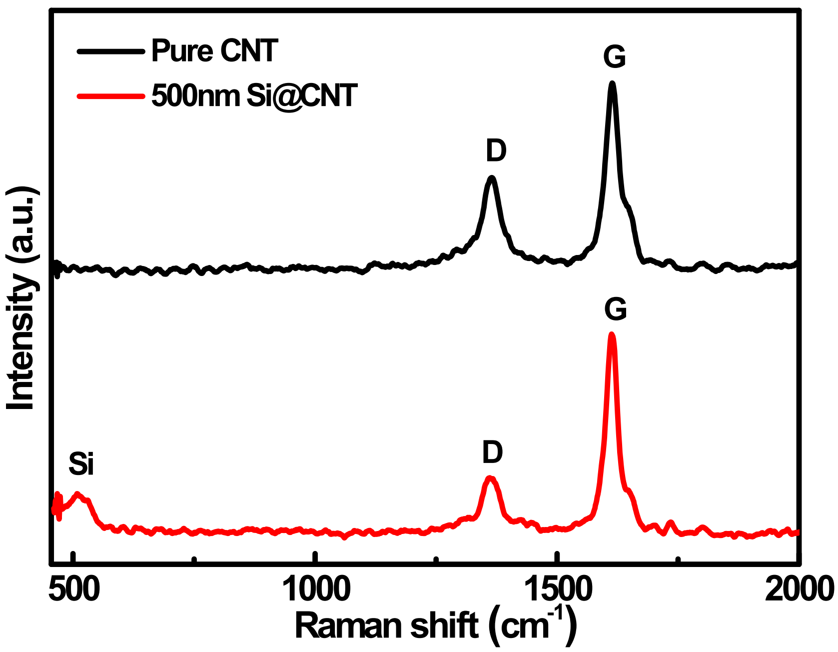

Fig. S1 Raman spectrum of the fresh CNT substrate with and without 500-nm Si film coating.

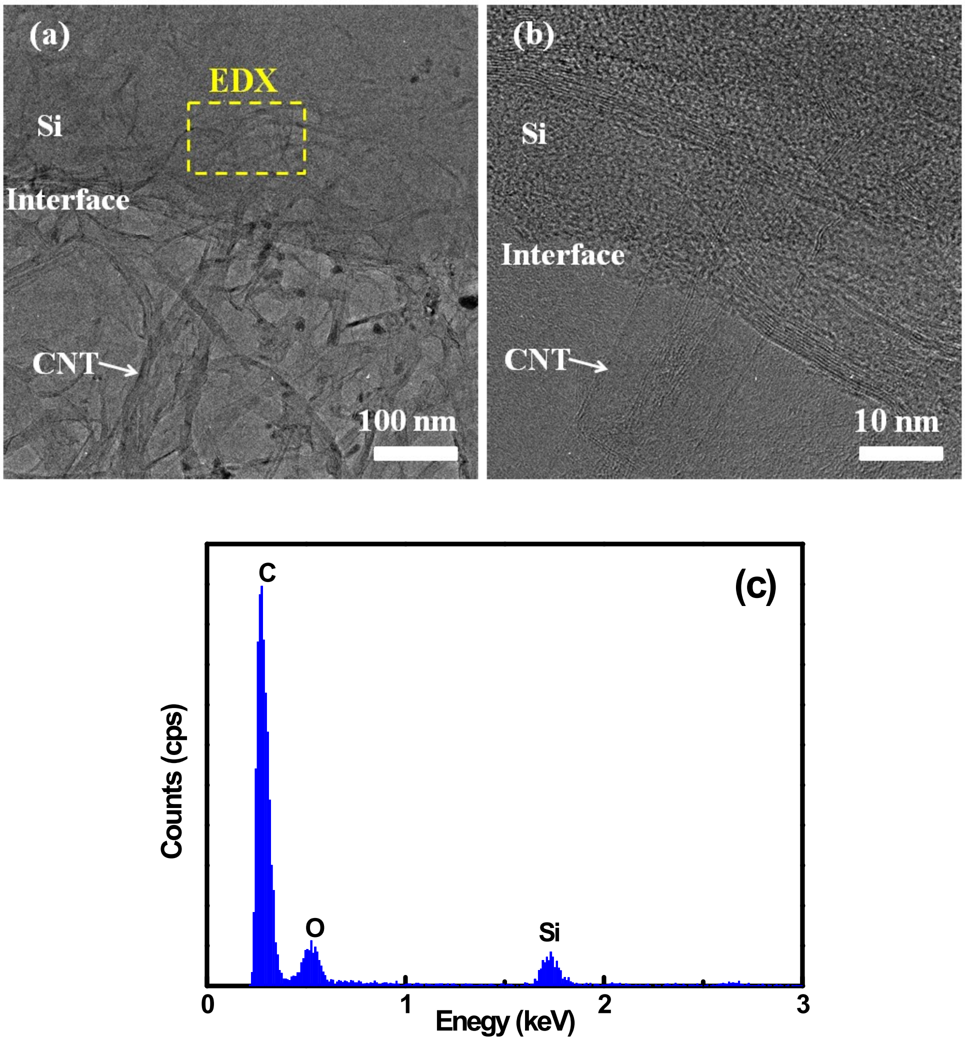

Fig. S2 (a) Low-resolution and (b) high-resolution TEM images near the Si/CNT interface for the fresh 500-nm Si@CNT anode. (c) EDX spectrum collected from the rectangular area in Fig. S2(a).

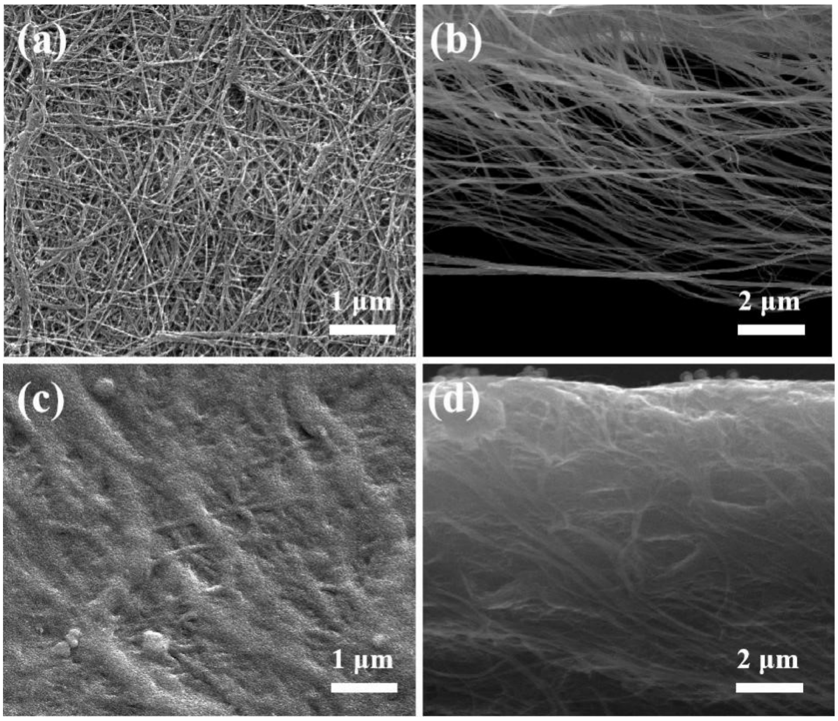

Fig. S3 (a) Plan-view and (b) cross-sectional SEM images of the fresh CNT anode. (c) Plan-view and (d) cross-sectional SEM images of the CNT anode after 100 cycles.

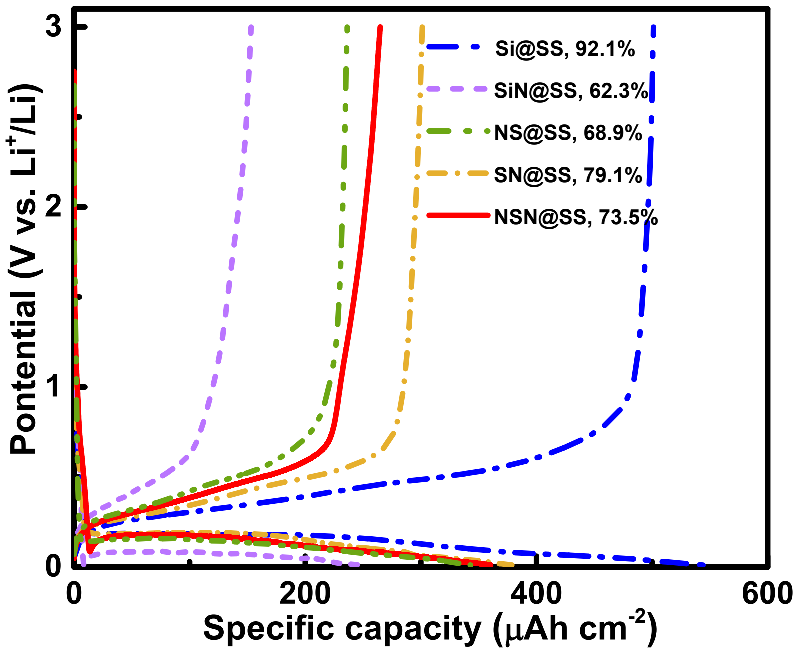

Fig. S4 Voltage profiles of the anodes on the stainless steel substrate in the initial cycle. The corresponding initial Coulombic efficiency of each anode is also shown. The active film is 500 nm if not otherwise specified.

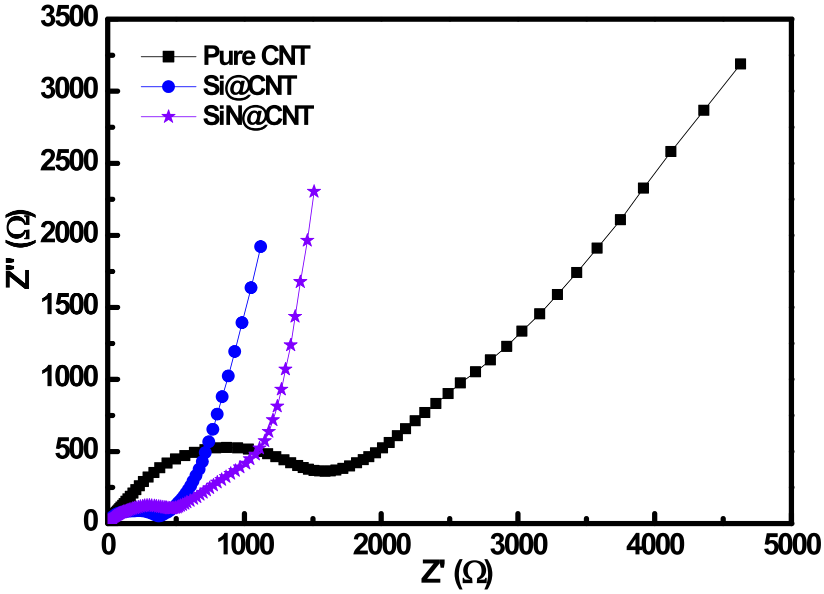

Fig. S5 Nyquist plots of the pure CNT, Si@CNT and SiN@CNT anodes under the fully charge state after electrochemical activation.

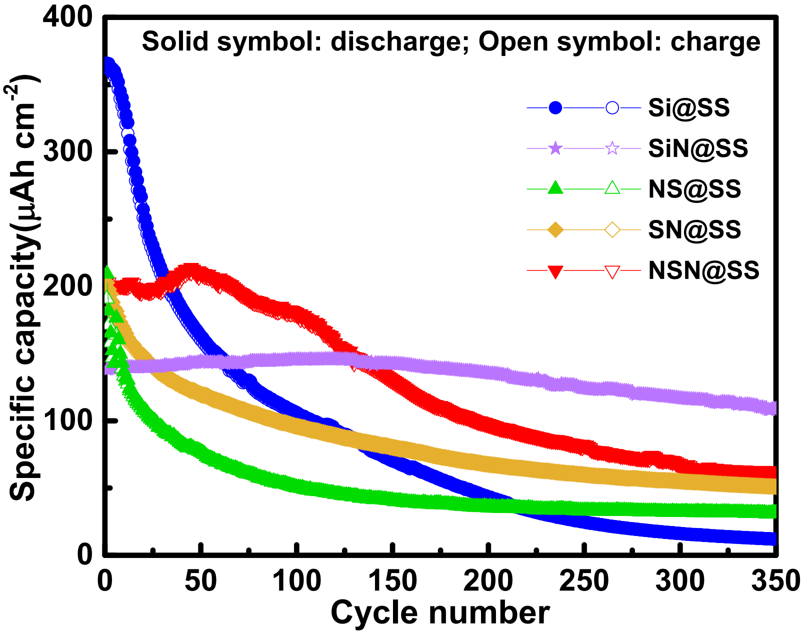

(a)

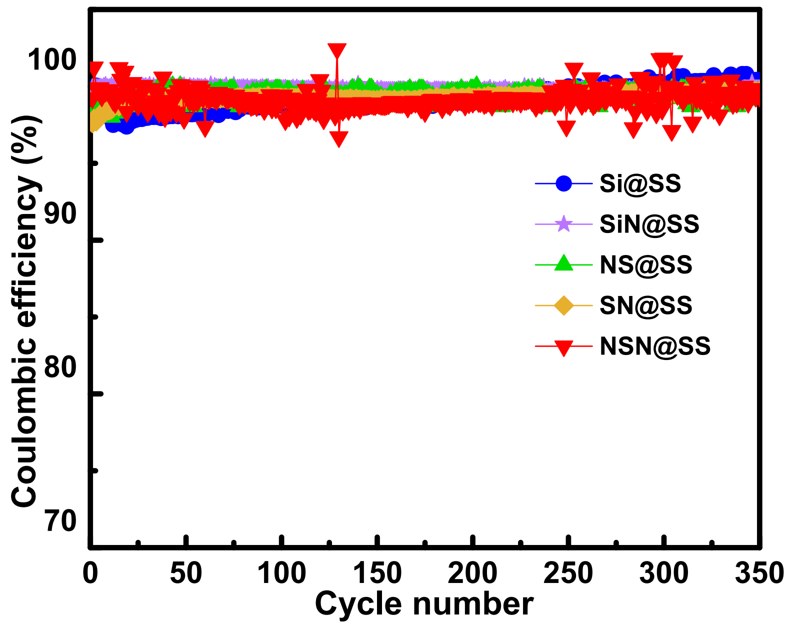

(b)

Fig. S6 (a) Cycling performance of the anodes on the stainless steel substrate at a current rate of 0.6 C. (b) The corresponding Coulombic efficiency with cycling. Note that the anodes are activated at a low current density of 0.01 C firstly before test.

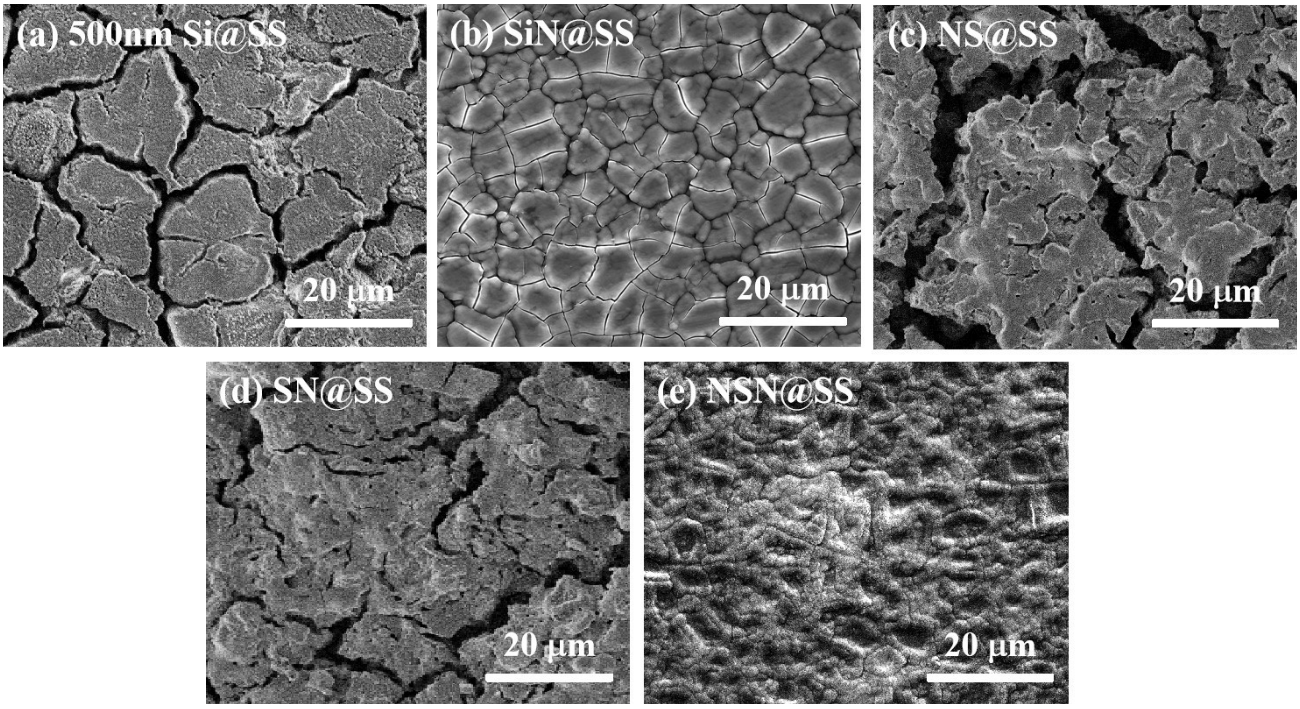

Fig. S7 SEM morphologies of the anodes on the stainless steel substrate after 100 cycles.

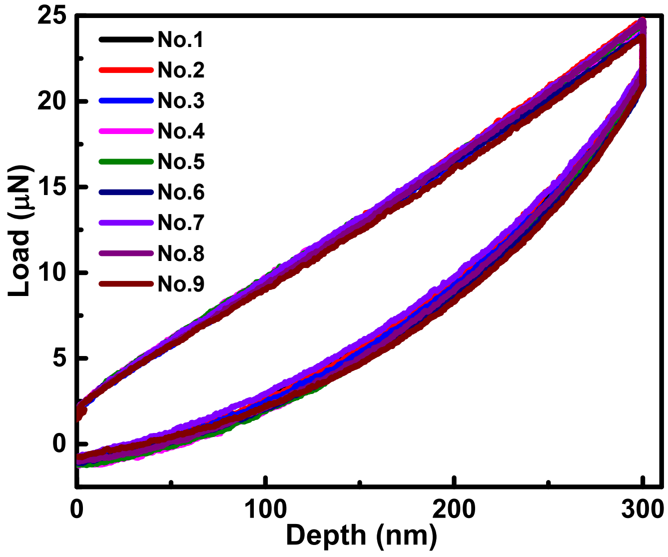

(a)

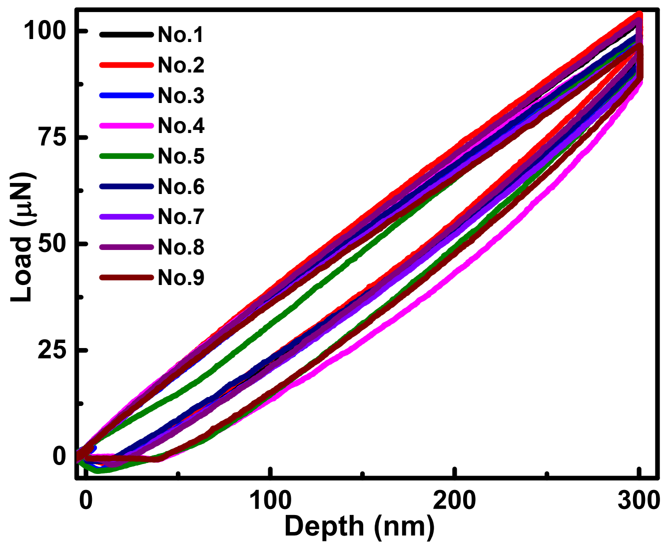

(b)

Fig. S8 Typical load-displacement curves of the CNT anode (a) before and (b) after 100 cycles by using nanoindentation. Nine points are measured for each sample. The hardness and elastic modulus can be extracted from the curves. The average elastic modulus/hardness are 110.6±4.4 MPa/13.4±1.2 MPa for the fresh CNT anode and 442.0±11.9 MPa/112.0±4.8 MPa for the cycled CNT anode.

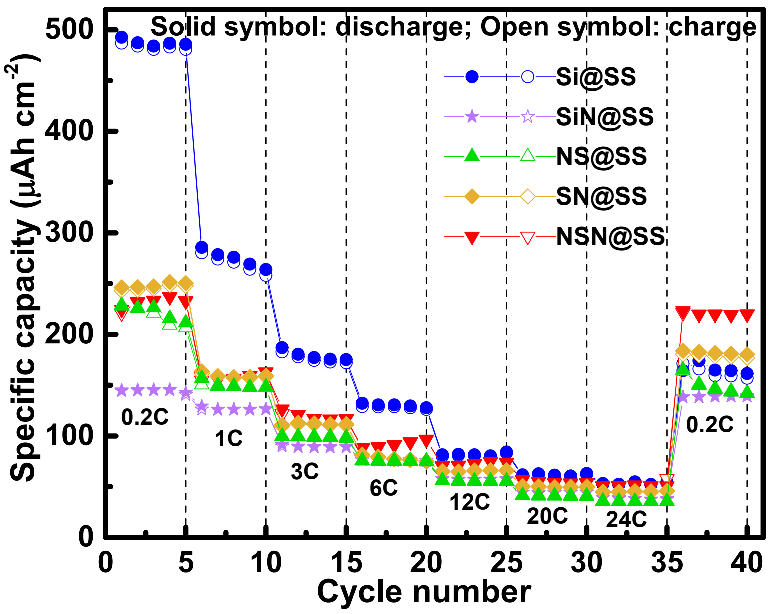

(a)

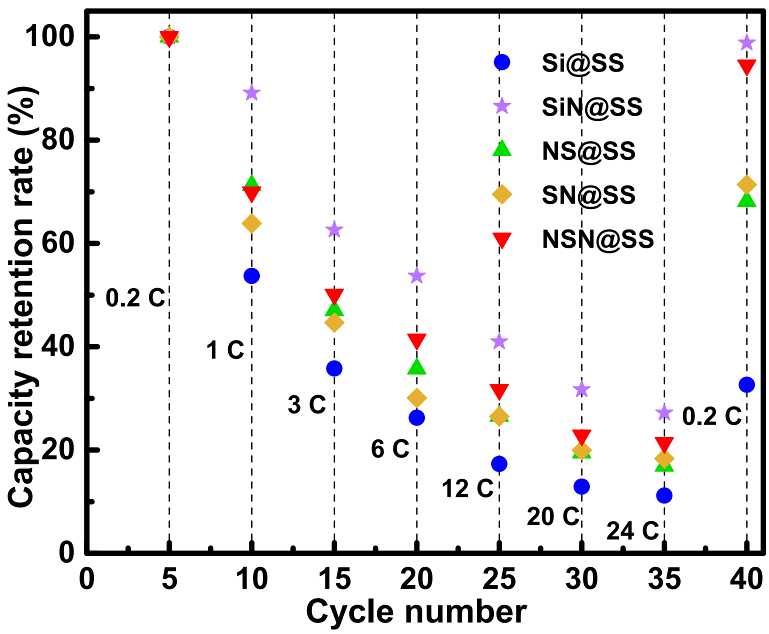

(b)

Fig. S9 (a) Rate performance of the anodes on the stainless steel substrate. (b) Capacity retention rate of each anode (defined as the ratio of the capacity at a given current rate to the capacity at 0.2 C). Note that the anodes are activated at a low current density of 0.01 C firstly before test.

Table S1. Performance comparison of the Si-based anodes in this work with other typical works reported in the literatures.

(Note: CNT: carbon nanotube; CVD: chemical vapor deposition; NW: nanowire; NP: nanoparticle; G: graphene; PVDF: Poly(vinylidene fluoride); PANi: polyaniline; NSN: SiN/Si/SiN.)

	Materials	Structures	Methods	Areal specific capacity (mAh/cm^2)	Cycling performance (charge loss rate per cycle, %)	Rate performance (retained capacity at high rate, %; retention recovery, %)	Ref
1	Si/Ni/PVDF	Si coated on flexible Ni/PVDF	Electrospinning +sputtering	0.42	0.04%	15.1% (20 C) 98.5% (0.2 C)	[1]
2	Si/C fiber paper	Si NPs on carbon fiber	Eectrospinning +Electrospray	1.19	0.08%	27.8% (3.6 C) 94.4% (0.1 C)	[2]
3	CNT/Si sheets	Si/CNT sheet	Rolling+CVD	0.71	0.6%	/	[3]
4	CNT/S/-C sheet	Carbon-coated CNT/Si sheet	Rolling+CVD	0.54	0.13%	58.1% (2 C) 78.5% (0.1 C)	[3]
5	Si/graphene paper	Si/graphene composite	Etching+ filtration	0.83	0.09%	39.3% (5 C) 95.2% (0.5 C)	[4]
6	CNT/Si film	CNT/Si composite	Ink +CVD	0.42	0.36%	83.3% (0.3 C) N/A (0.1 C)	[5]
7	Si NP/PANi	Si/PANi composite	In-situ polymerization	0.38	0.002%	44.0%(2 C) 84.0% (0.1 C)	[6]
8	Si NW arrays	Si NW array	Template +CVD	0.13	0.22%	29.1% (10 C) N/A(0.2 C)	[7]

9	**t-Si@G NW array**	**Free-standing textured Si@graphene carbon nanowire array**	**Metal-assisted chemical etching +CVD**	**0.38**	**0.13%**	**28.6% (3 C) 91.4%(0.2 C)**	**[8]**
10	**Si membrane**	**Si membrane structure with 3D configuration**	**Template +CVD**	**0.06**	**0.18%**	**38.85% (8 C) N/A (0.1 C)**	**[9]**
11	**DWSiNT**	**Double-walled Si/SiOx nanotube**	**Template +CVD**	**0.18**	**0.03%**	**45.0% (10 C) 83.3% (1 C)**	**[10]**
12	**Si conductive nanopaper**	**Si/CNT conductive nanopaper**	**Template +CVD**	**0.1**	**0.23%**	**58.1% (2 C) 90.3% (0.1 C)**	**[11]**
13	**Si NP/C**	**Si NP deposited on a porous carbon current collector**	**Customized CVD with expanding thermal plasma source**	**1.2**	**0.25%**	**16.7% (6 C) 66.7% (0.1 C)**	**[12]**
14	**Si/Ge hNWs**	**Axial Si/Ge Heterostructure Nanowires**	**CVD**	**0.17**	**0.09%**	**36.8% (10 C) 95.0% (0.1 C)**	**[13]**
15	**Si/G/GF**	**Hierarchical graphene-scaffolded silicon/graphite composite**	**Ball-milling + self-assembly**	**0.62**	**0.07%**	**22.7% (15 C) 93.4% (0.5 C)**	**[14]**
16	**NSN@CNT**	**Symmetrical sandwich-structured NSN composite on CNT paper**	**CVD**	**0.53**	**0.07%**	**28.4% (12C) 23.8% (20 C) 96.8% (0.2 C)**	**This work**
17	**Si@CNT**	**Si film on CNT paper**	**CVD**	**0.59**	**0.19%**	**14.8% (20 C) 38.3% (0.2 C)**	**This work**

References

[1] Q. Xiao, Q. Zhang, Y. Fan, X. Wang, R. A. Susantyoko, *Energ Environ Sci*. **2014**, 7, 2261.

[2] Y. Xu, Y. Zhu, F. Han, C. Luo, C. Wang, *Adv Energy Mater*. **2015**, 5, 1400753.

[3] K. Fu, O. Yildiz, H. Bhanushali, Y. Wang, K. Stano, L. Xue, X. Zhang, P. D. Bradford, *Adv. Mater*. **2013**, 25, 5109.

[4] H. Jiang, X. Zhou, G. Liu, Y. Zhou, H. Ye, Y. Liu, K. Han, *Electrochim. Acta*. **2016**, 188, 777.

[5] L. Cui, L. Hu, J. W. Choi, Y. Cui, *Acs Nano*. **2010**, 4, 3671.

[6] H. Wu, G. Yu, L. Pan, N. Liu, M. T. McDowell, Z. Bao, Y. Cui, *Nat Commun*. **2013**, 4, 1943.

[7] J. H. Cho, S. T. Picraux, *Nano Lett.* **2013**, 13, 5740.

[8] B. Wang, X. Li, T. Qiu, B. Luo, J. Ning, J. Li, X. Zhang, M. Liang, L. Zhi, *Nano Lett.* **2013**, 13, 578.

[9] F. Xia, S. B. Kim, H. Cheng, J. M. Lee, T. Song, Y. Huang, J. A. Rogers, U. Paik, W. I. Park, *Nano Lett.* **2013**, 13, 3340.

[10] H. Wu, G. Chan, J. W. Choi, I. Ryu, Y. Yao, M. T. McDowell, S. W. Lee, A. Jackson, Y. Yang, L. Hu, Y. Cui, *Nat Nanotechnol*. **2012**, 7, 310.

[11] L. Hu, N. Liu, M. Eskilsson, G. Zheng, J. McDonough, L. Wågberg, Y. Cui, *Nano Energy*. **2013**, 2, 138.

[12] Y. Xu, E. Swaans, S. Chen, S. Basak, P. P. R. M. L. Harks, B. Peng, H. W. Zandbergen, D. M. Borsa, F. M. Mulder, *Nano Energy*. **2017**, 38, 477.

[13] K. Stokes, G. Flynn, H. Geaney, G. Bree, K. M. Ryan, *Nano Lett.* **2018,** 18, 5569.

[14] S. Zhu, J. Zhou, Y. Guan, W. Cai, Y. Zhao, Y. Zhu, L. Zhu, Y. Zhu, Y. Qian, *Small*. **2018**, 14, e1802457.